Varying Excitation Conditions in a Multi-component Submillimeter Galaxy

Chelsea E. Sharon[1], Andrew J. Baker[1], Andrew I. Harris[2], Linda J. Tacconi[3], Dieter Lutz[3], & Steven N. Longmore[4]

Image courtesy of NRAO/AUI

[1]Rutgers, the State University of New Jersey [2]University of Maryland
[3]Max-Planck-Institut für extraterrestrische Physik [4]European Southern Observatory

CO in Submillimeter Galaxies

- CO is a valuable tracer of the molecular gas that fuels star formation.
- Radiative transfer modeling of CO lines tells us about the physical conditions of the molecular gas (e.g., using the Large Velocity Gradient approximation; Ward et al. 2003; Weiß et al. 2007).
- Recent CO observations indicate that submillimeter galaxies (SMGs) have a common CO(3-2)/CO(1-0) line ratio of $R_{3,1}$≈0.6 (in brightness temperature units; e.g., Swinbank et al. 2010; Harris et al. 2010; Ivison et al. 2011; Danielson et al. 2011).
- This line ratio indicates that the molecular ISM of SMGs has multiple phases, including a substantial cold gas reservoir (best traced by the CO(1-0) line).

SMM J00266+1708

- Detected with SCUBA Lens Survey (Smail et al. 2002).
- Initial CO observations failed due to an incorrect optically-determined redshift (Frayer et al. 2000).
- Observations of the CO(1-0) line with the Zpectrometer (Harris et al. 2008) on the Robert C. Byrd Green Bank Telescope confirmed a *Spitzer* PAH redshift estimate (Valiante et al. 2007) of z=2.742 (Baker et al. in prep.).
- We followed up our Zpectrometer detection at the Expanded Very Large Array in CO(1-0), at the Plateau de Bure Interferometer in CO(3-2) and CO(5-4), and at the Submillimeter Array in CO(7-6) (Sharon et al. in prep.).

The Zpectrometer opened up in lab at UMD.

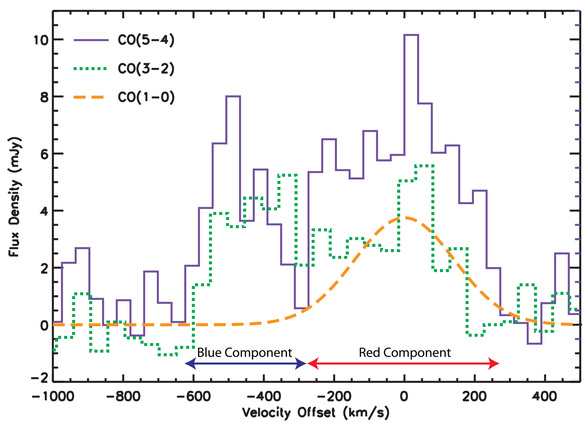

Figure 1- The CO(5-4) (solid/purple) and CO(3-2) (dotted/green) spectral lines, shifted to match the rest frame velocity of the CO(1-0) line (Gaussian fit to GBT observation shown in dashed orange line; multiplied by a factor of five for clarity).

Evidence for Multiple Components:

- The high SNR CO(5-4) spectrum shows a strong division and asymmetry between the two peaks, which is unlikely for a rotating disk.
- Channel maps of the blue peak are spatially coincident and separate from the redder channels, which (for the CO(3-2) line) show a clear velocity gradient along a position angle of ~70°.
- Line ratio differences indicate the two components have different excitation conditions, which is unlikely if they are physically associated.

Multiple Components

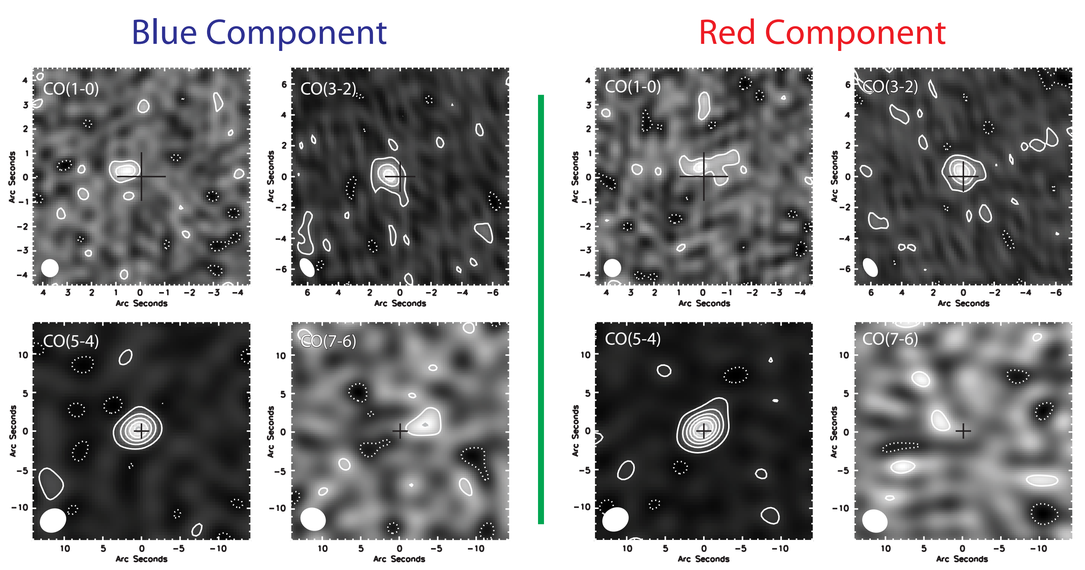

Figure 2- Integrated line maps for the blue component (left) and red component (right). For each component, the maps are of the CO(1-0) (top left), CO(3-2) (top right), CO(5-4) (bottom left), and CO(7-6) (bottom right) lines. The center cross marks the position and astrometric uncertainty of the Frayer et al. (2000) continuum detection (scaled up by a factor of five for clarity). Beam sizes are shown in the lower left corners. The lowest contours are at ±2σ for all maps (negative contours are dotted), but the contour spacings are multiples of 2σ, 4σ, 4σ, and 2σ for the CO(1-0), CO(3-2), CO(5-4), and CO(7-6) maps, respectively.

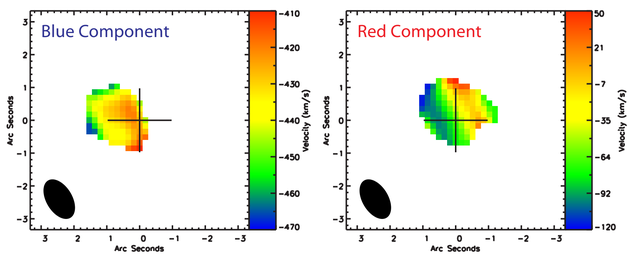

Figure 3- The CO(3-2) first moment maps of the blue component (left) and red component (right). The center cross marks the positions and astrometric uncertainty of the Frayer et al. (2000) continuum detection (scaled up by a factor of five for clarity). Pixels with values <3σ in the corresponding integrated line map have been blanked out. Beam sizes are given in the lower left corners.

Additional Details:

- The CI $^3P_2$->$^3P_1$ fine structure line is marginally detected for the red component at 3.75σ (2.44 ± 0.49 Jy km s^{-1}).
- The only significant continuum detection is at 1mm (SMA); S_{1mm}= 5.34 ± 1.07 mJy.
- Fits to the resolved CO(3-2) line give radii of 2.9 kpc and 3.8 kpc for the blue and red components, and a separation distance of 5.8 kpc.
- The EVLA observations show evidence for extended emission in the red component, though it is likely partially resolved out.
- Apparent flips in the red component velocity gradient (Fig. 3) are from the large spatial extent of the two strongly peaked channels (Fig. 1).

Excitation Analysis Methods:

- Our measured line ratios are compared to a single-phase radiative transfer model using the large velocity gradient (LVG) approximation.
- The LVG model was adapted from Ward (2002) to include the effects of the CMB (which can excite CO to low J levels at high z).
- The three input parameters required to model the line ratios are the kinetic temperature, the H_2 density, and the CO column density per unit velocity gradient.
- The parameter space is sampled evenly in temperature (excluding T<T_{CMB}), and evenly in the logarithm of H_2 density and CO column density per unit velocity gradient.
- Bayesian techniques from Ward et al. (2003) are used to assess the likelihood of a particular input parameter triplet resulting in the measured CO spectral line energy distribution (CO SLED).
- The prior probability is assumed to be uniform for temperature, and uniform in the logarithm for H_2 density and for CO column density per unit velocity gradient.
- The two components are treated separately.
- This method can be generalized to include multiple phases by adding each phase's contribution to the line flux in proportion to their filling factor ratios (Ward et al. 2003).

Varying Excitation Conditions

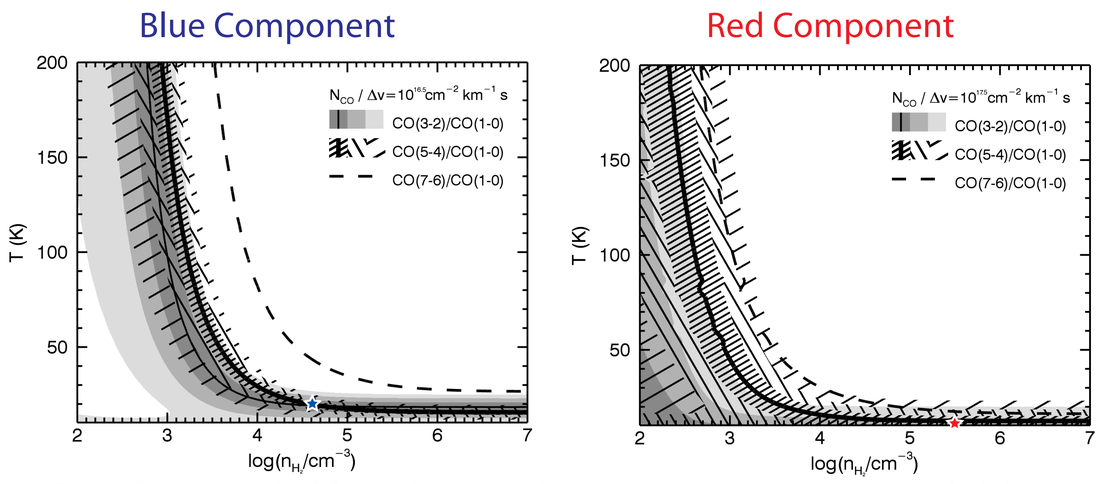

Figure 4- Contour plot of the LVG model showing where the predicted line ratios match our measurements for the blue component (left) and red component (right). The thin and thick solid lines are the measured CO(3-2)/CO(1-0) and CO(5-4)/CO(1-0) line ratios where the 1σ, 2σ, and 3σ uncertainties are marked with lighter shades of gray and sparser hash marks, respectively. The dashed line is the 3σ upper limit of the CO(7-6)/CO(1-0) line ratio; regions of the parameter space below and to the left of that line are within the limit. The stars mark the best fit CO SLEDs in Fig. 5.

Table 1: SMM J00266+1708 Line Ratios

Component	$R_{7,5}$	$R_{7,3}$	$R_{7,1}$	$R_{5,3}$	$R_{5,1}$	$R_{3,1}$
Total	< 0.44	< 0.28	< 0.21	0.63 ± 0.11	0.48 ± 0.12	0.77 ± 0.17
Blue	< 0.97	< 0.44	< 0.38	0.45 ± 0.08	0.39 ± 0.07	0.87 ± 0.12
Red	< 0.47	< 0.35	< 0.16	0.75 ± 0.14	0.34 ± 0.08	0.45 ± 0.10

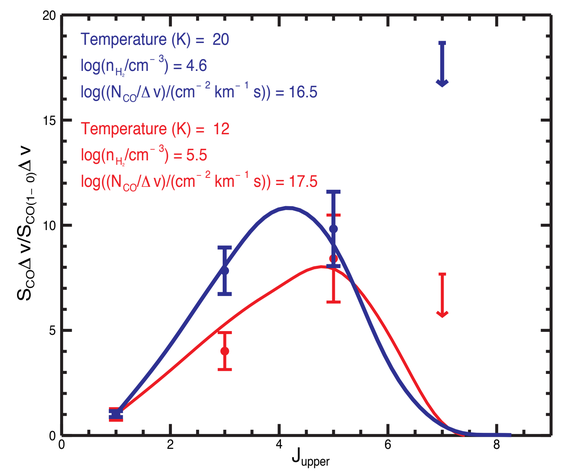

Figure 5- Best fit single-phase CO SLEDs for the blue and red components (solid lines) and the measured line ratios (points; not in brightness temperature units).

Differing Phases:

- The blue component line ratios are consistent with a single-phase molecular ISM.
- $R_{3,1}$ for the blue component is more similar to that of quasar host galaxies ($R_{3,1}$≈1.0; Riechers et al. 2011) than that of SMGs.
- The red component line ratios are *not* consistent with a single-phase molecular ISM.
- $R_{3,1}$ for the red component is comparable to, though less than, that of other SMGs.

Conclusions

While the average excitation properties of SMM J00266+1408 (as probed by $R_{3,1}$) are consistent with those of other SMGs, a detailed analysis reveals a much more complicated system; it is unclear how common such systems are among the SMG population.

SMM J00266+1708 is a clear example of a major merger at high redshift, showing two interacting systems with stark differences in their dynamical structure and excitation conditions (see also Engel et al. 2010).

Both the total system and the red component of SMM J00266+1708 demonstrate the need for a detailed multi-phase analysis of the physical conditions in SMGs.

The dynamical and molecular gas masses of the two components are somewhat contradictory (especially when using the revised line luminosity to gas mass conversion factor of Harris et al. 2010), but this is common for SMGs, and reinforces the need for more exploration on the choice of conversion factor.

RUTGERS UNIVERSITY

The authors acknowledge support from NSF grants AST-0503946 and AST-0708653, and Steve Sirisky for his contributions to the LVG code.

References: Baker, A. J. et al. 2012 (in preparation); Danielson, A. L. R. et al. 2011, MNRAS, 410, 1687; Engel, H. et al. 2010, ApJ, 724, 233; Frayer, D. T. et al. 2000, AJ, 120, 1668; Harris, A. I. et al. 2010, ApJ, 723, 1130; Ivison, R. J. et al. 2011, MNRAS, 412, 1913; Riechers, D. A. et al. 2011, ApJL, 739, 32; Sharon, C. E. et al. 2012 (in preparation); Smail, I. et al. 2002, MNRAS, 331,495; Swinbank, A. M. et al. 2010, Nature, 464, 733; Valiante E. et al. 2007, ApJ, 660, 1060; Ward, J. S. 2002, PhD Thesis; Ward, J. S. et al. 2003, ApJ, 587, 171; Weiß, A. et al. 2007, ASPCS, 375, 25